

# Wear Behaviour of Alumina and Sialon in Line Contact Lubricated with Diamond Slurry

E. Jisheng,<sup>a</sup> T. A. Stolarski,<sup>a\*</sup> & D. T. Gawne<sup>b</sup>

<sup>a</sup>Department of Mechanical Engineering and <sup>b</sup>Department of Materials Technology, Brunel University, Uxbridge, Middlesex UB8 3PH, UK

(Received 5 April 1995; revised version received 6 November 1995; accepted 13 November 1995)

## Abstract

*Investigation into the wear behaviour of alumina and sialon was carried out in the line contact configuration lubricated with diamond slurry. The experiments were conducted using different counterface materials, contact loads and size of the diamond abrasive particles in the slurry. The results indicate that the material removal rate depends significantly on the action of the diamond particles and counterface material. Both contact conditions facilitate easy ingress of diamond particles into the interface and the ability of the counterface material to entrap diamond particles contributes to a high rate of material removal.*

## 1 Introduction

Engineering ceramics have found use in many applications, such as engine parts, ball bearings, artificial bone and hip replacements and gyroscopes, because of their good chemical inertness, hardness, high temperature stability and very good wear resistance. These advantages, however, are somewhat compromised by the difficulties in their processing. An example in question is the extremely low material removal rate during conventional grinding, which obviously makes surface finishing processes of ceramics an expensive operation. Increasing use of ceramics in a variety of applications has created a need for better understanding of the mechanisms involved in the grinding process so that an effective grinding method can be developed.

There are many methods of grinding of ceramics. Creep feed grinding, ultrasonic-assisted grinding, energy-beam-assisted grinding, magnetic fluid grinding all serve as examples. However, the dominant and most effective commercial current practice remains diamond slurry grinding.<sup>1</sup> Many

researchers have paid a lot of attention to the mechanism of material removal during grinding.<sup>2–4</sup> In the diamond slurry grinding process, some of the key factors responsible for the increase in the material removal rate may be considered in terms of the action of the diamond particles and the characteristics of the counterface materials. Kato<sup>5</sup> studied the grinding process using a rolling contact configuration and a magnetic fluid containing diamond particles. His results show that the material removal rate is almost 40 times higher than that achievable in a non-magnetic environment. Childs *et al.*<sup>6</sup> found that this high material removal rate results from a considerable amount of skidding taking place within the contact region. Stolarski *et al.*<sup>7</sup> pointed out that the high material removal rate occurs when the abrasive action of diamond particles is a dominant mechanism.

In this paper the results of a study into the factors controlling the material removal rate during model grinding experiments are presented. The emphasis is on the understanding of the relationships between effectiveness of material removal and the characteristics of ceramic, counterface material, contact sliding conditions, and the composition of diamond slurries.

## 2 Experimental Conditions

### 2.1 Grinding tester

All the tests described in this paper were carried out in the modified Falex machine. Figure 1 shows a ceramic sample together with counterface elements and all dimensions relevant to the experiments reported here. In the configuration used during the experiments presented in this paper, a ceramic specimen in the form of a pin (6.5 mm nominal diameter and 25.4 mm long) was attached to the shaft driven by an electric motor. The specimen was in line contact with two V-shaped blocks and the load on the contact was applied through the

\*To whom correspondence should be addressed.

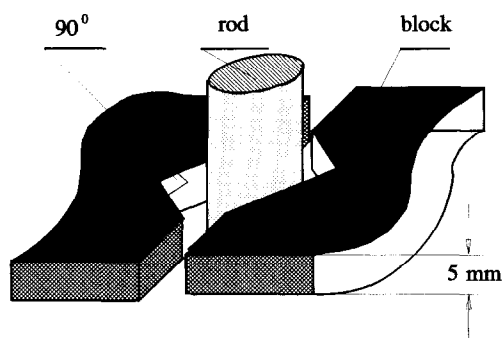


Fig 1. Contact configuration used during the grinding experiments.

blocks. The length of the contact was 5 mm. Both ceramic specimen and V-shaped blocks were submerged in the diamond slurry contained in a specially shaped container. To prevent sedimentation of diamond particles a small stirrer was attached to the ceramic specimen, as there was no magnetic field which could help keep the abrasive particles in suspension.

## 2.2 Materials

Two types of ceramic, namely sialon and alumina, were tested. Both ceramic materials were supplied as rods 6.5 mm in diameter and 10 mm long. Three different materials were used for the V-shaped blocks: they were mild steel, brass and aluminium alloy. However, the majority of testing was carried out using steel V-blocks. Oil-based diamond slurries with four sizes of diamond particles, namely 1, 6, 15 and 25  $\mu\text{m}$ , were used throughout the experiments.

## 2.3 Experimental procedure

All experiments were carried out at the speed of 300 rev min<sup>-1</sup>. The amount of slurry placed in the container was 20 ml and was sufficient to submerge completely the contact between the ceramic rod and the V-shaped counterfaces. The required speed of the ceramic specimen was attained first, then the load on the contact was carefully applied. The load on the contact ranged from 135 to 900 N. The duration of a typical test was 60 min. The temperature in close proximity to the contact zone was continuously monitored using a thermocouple placed at the trailing edge of one of the V-blocks. Before each test all experimental pieces, i.e. specimen, V-shaped blocks and the container, were ultrasonically cleaned in acetone. Both ceramic specimen and V-blocks were weighed before and after the test to obtain an estimate of the rate of material removal. The rate of material removal is expressed as a volume loss of material per unit time calculated on the basis of weight measurements.

## 2.4 Surface analyses

Scanning electron microscopy (SEM) was used to examine the appearance of the ceramic surface, debris produced during the test and the V-blocks. Optical microscopy was used to examine the metallurgical microstructure of the V-blocks.

## 3 Results

### 3.1 Alumina experiments

#### 3.1.1 Effect of applied load and diamond particle size

Results obtained during tests on alumina in contact with steel V-blocks are presented in Fig. 2. In this figure the rates of material removal are plotted against the load on contact for different sizes of diamond particles. The first observation to be made is that the material removal rate increases with the applied load for all sizes of diamond particles. For diamond particle sizes of 1, 15 and 25  $\mu\text{m}$  the change in material removal rate with load is linear. In the case of 6  $\mu\text{m}$  diamond particles, a clear transition in the material removal rate occurring at a load of 450 N can be seen.

The rate of material removal also increases with the size of diamond particles. This is true for 1, 6 and 15  $\mu\text{m}$  diamond particles. A maximum rate of material removal is found to be for 15  $\mu\text{m}$  particles. Further increase in diamond particle size brings about a substantial decrease in material removal rate. In fact, under the load of 675 N, the rate of material removal for 25  $\mu\text{m}$  diamond particles is almost 20 times lower than that recorded for 15  $\mu\text{m}$  particles and approximately five times lower than the removal rate for 1  $\mu\text{m}$  particles.

In Fig. 3 the temperature, recorded by the thermocouple located at the trailing edge of the V-shaped block, is presented in a function of applied load for all four sizes of diamond particles used. It is seen that the temperature increases steadily with

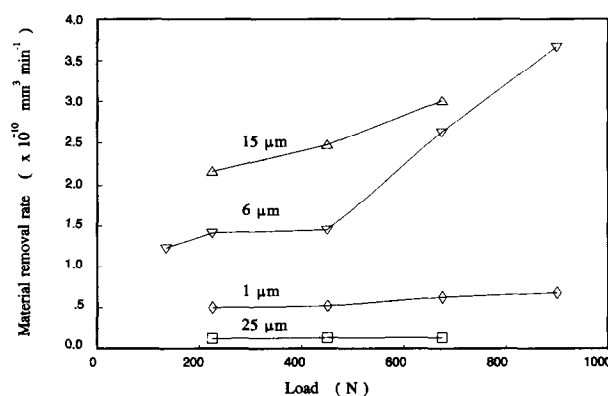


Fig. 2. Material removal rate of alumina as a function of the applied load for different sizes of diamond particles in the slurry. Rotational velocity of the ceramic pin, 300 rev min<sup>-1</sup>; duration of the test, 60 min.

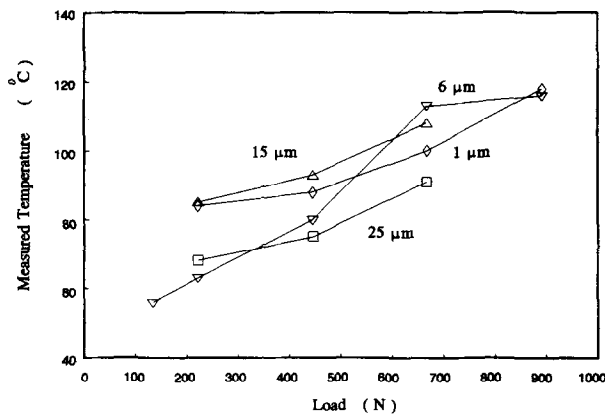


Fig. 3. Temperature within the contact zone as a function of the applied load for alumina and different sizes of diamond particles in the slurry. Rotational velocity of the ceramic pin, 300 rev min<sup>-1</sup>; duration of the test, 60 min.

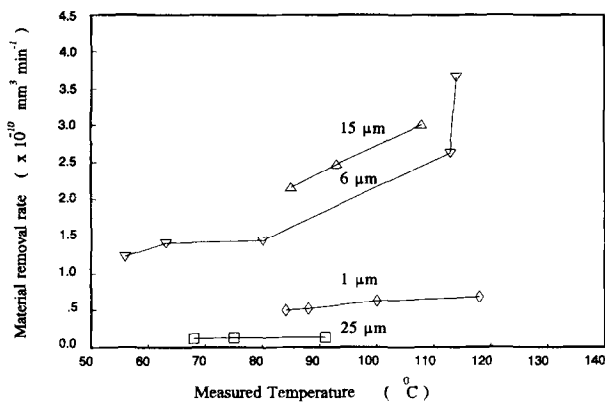


Fig. 4. The relationship between material removal rate and contact temperature for alumina and different sizes of diamond particles in the slurry. Rotational velocity of the ceramic pin, 300 rev min<sup>-1</sup>; duration of the test, 60 min.

the applied load for all sizes of diamond particles used. The highest temperatures were recorded for 15 μm diamond particles followed by 1 μm and 25 μm. The temperature rise during grinding in the presence of 6 μm particles is the lowest up to a load of 300 N, thereafter a very fast increase in temperature with load was observed. At 675 N the temperature for 6 μm particles is the highest.

The relationship between temperature within the contact and the rate of material removal is shown in Fig. 4. It is seen that high rates of material removal are associated with relatively high temperatures. However, this relationship is strongly influenced by the size of the diamond particles.

### 3.1.2 Effect of counterface material

To examine the effect of counterface material on the efficiency of grinding, V-blocks made of mild steel, aluminium alloy and brass were used during experiments in 6 μm diamond slurry. Figure 5 shows the results obtained. The highest material

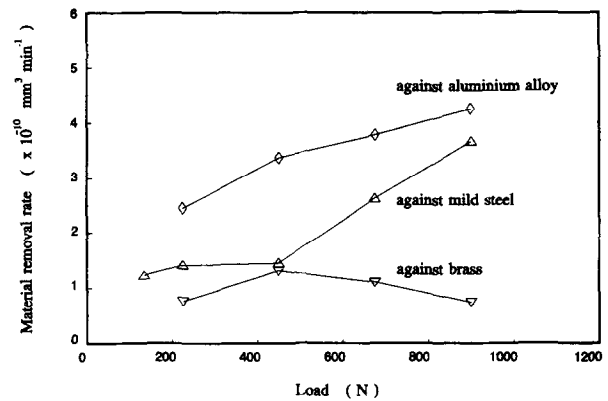


Fig. 5. Variation in the alumina removal rate with the applied load for different counterface materials. Diamond slurry with 6 μm particles; rotational velocity of the ceramic pin, 300 rev min<sup>-1</sup>; duration of the test, 60 min.

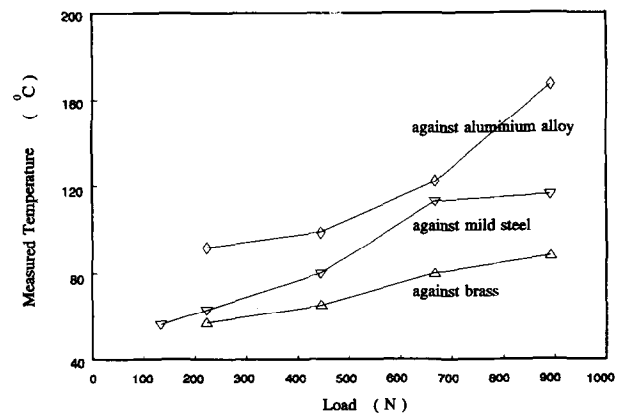


Fig. 6. Temperature within the contact zone as a function of the applied load for alumina and different counterface materials. Diamond slurry with 6 μm particles; rotational velocity of the ceramic pin, 300 rev min<sup>-1</sup>; duration of the test, 60 min.

removal rates were obtained for the aluminium alloy over the whole range of applied loads. The lowest rates were recorded for brass, therefore no more experiments were carried out with V-blocks made of brass. Mild steel produced removal rates

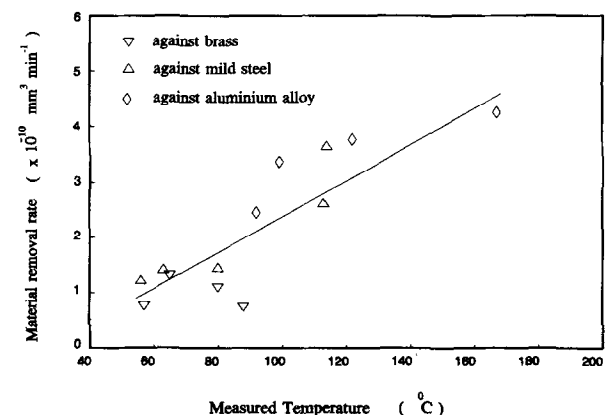


Fig. 7. The relationship between material removal rate and contact temperature for alumina and different counterface materials. Diamond slurry with 6 μm particles; rotational velocity of the ceramic pin, 300 rev min<sup>-1</sup>; duration of the test, 60 min.

somewhere between these two. This finding points to the importance of retention of abrasive particles within the contact region. It appears that aluminium alloy is the material into which the diamond particles could embed more easily, compared with the other two materials used.

Variations in the contact temperature for all three counterface materials are presented in Fig. 6, while the relationship between contact temperature and the rate of material removal is shown in Fig. 7.

### 3.2 Sialon experiments

#### 3.2.1 Effect of diamond particles size

The removal rates of sialon for different sizes of diamond particles were investigated at constant load of 900 N. Figure 8 shows the results for mild steel and aluminium alloy counterfaces. It is interesting to note that the maximum rate for the mild steel counterface was achieved when 6  $\mu\text{m}$  diamond particles were used. In the case of the aluminium alloy counterface, the maximum removal rate was obtained for 15  $\mu\text{m}$  diamond particles. Both

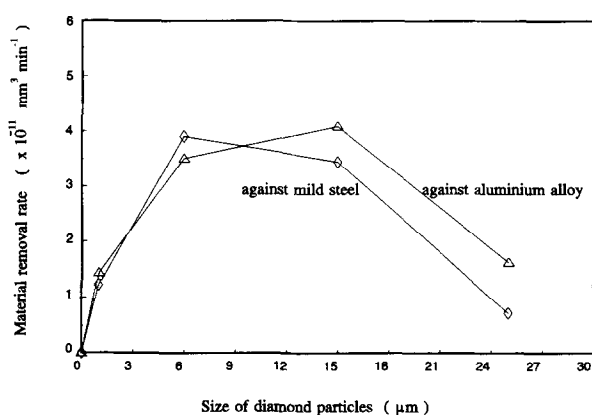


Fig. 8. Sialon removal rate as a function of diamond particles size for different counterface materials. Rotational velocity of the ceramic pin, 300 rev  $\text{min}^{-1}$ ; duration of the test, 60 min.

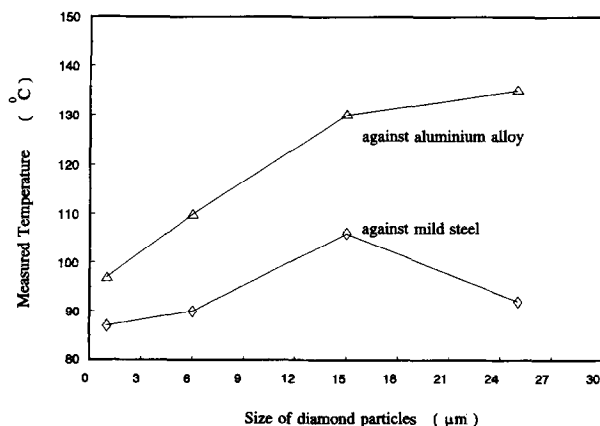


Fig. 9. Temperature within the contact zone as a function of the size of diamond particles in the slurry for different counterface materials. Ceramic material, sialon; rotational velocity of the ceramic pin, 300 rev  $\text{min}^{-1}$ ; duration of the test, 60 min.

maximum removal rates are of the same magnitude. The temperatures within the contact area are substantially higher for the aluminium alloy counterface than for the mild steel, as evidenced by the results shown in Fig. 9. For the aluminium alloy counterface the temperature rises steadily with increasing size of the diamond particles. This is not the case for the mild steel counterface where a clear maximum exists. This maximum occurs for 15  $\mu\text{m}$  diamond particles.

#### 3.2.2 Effect of applied load

To find the load at which the rate of material removal is at its highest, grinding experiments on sialon were carried out in 15  $\mu\text{m}$  diamond slurry using both aluminium alloy and mild steel counterfaces. Figure 10 shows the material removal rate plotted against the applied load. Both counterface materials used produce almost linear increase in the material removal rate with increasing load. Again, the aluminium alloy counterface proved to be more effective in material removal than the mild steel counterface under nominally the same

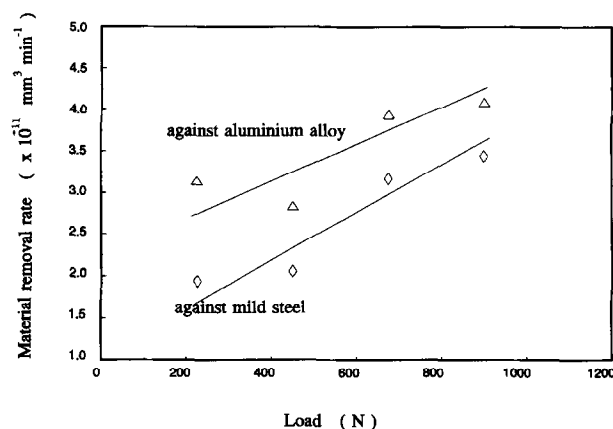


Fig. 10. Sialon removal rate as a function of the applied load for mild steel and aluminium alloy as counterface materials. Diamond slurry with 15  $\mu\text{m}$  particles; rotational velocity of the ceramic pin, 300 rev  $\text{min}^{-1}$ ; duration of the test, 60 min.

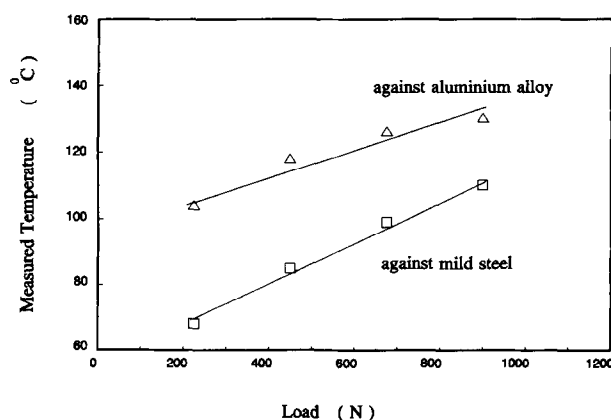


Fig. 11. Temperature within the contact zone as a function of the applied load for sialon in contact with mild steel and aluminium alloy counterface. Diamond slurry with 15  $\mu\text{m}$  particles; rotational velocity of the ceramic pin, 300 rev  $\text{min}^{-1}$ ; duration of the test, 60 min.

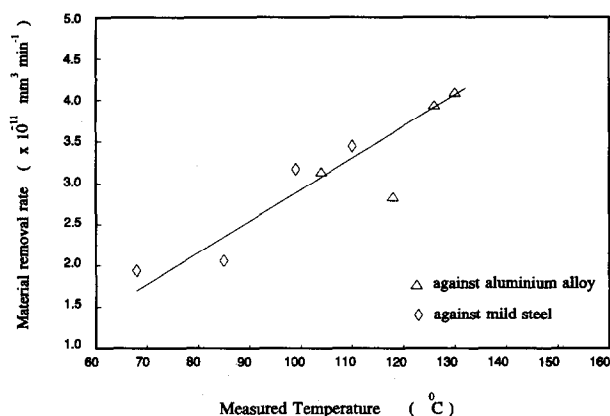


Fig. 12. Relationship between sialon removal rate and contact temperature for mild steel and aluminium alloy counterface. Diamond slurry with 15  $\mu\text{m}$  particles; rotational velocity of the ceramic pin, 300 rev min<sup>-1</sup>; duration of the test, 60 min.

test conditions. Temperature variations with applied load for both counterface materials used are shown in Fig. 11. The change in temperature with applied load is linear and higher temperatures were recorded for the aluminium counterface. The relationship between material removal rate and temperature within the contact is also linear for both counterface materials used (see Fig. 12).

## 4 Discussion

### 4.1 Transition from high to low material removal rate

In general, the rate of material removal of alumina increases linearly with increase in the applied load for 1, 15 and 25  $\mu\text{m}$  diamond particles. However, the alumina removal rate in 6  $\mu\text{m}$  diamond slurry shows a clear transition at a load of 450 N, as shown in Fig. 2. This transition can be explained in terms of the ability of the different sized abrasive particles to embed themselves into the steel counterface under a given load. It appears that, under loads of 450 N and above, 15  $\mu\text{m}$  abrasive particles were able to anchor themselves permanently into the counterface, hence the observed transition in material removal rate. To clarify this behaviour further, microscopy studies of the ceramic microstructure resulting from grinding tests were undertaken. Figure 13(a) shows the appearance of alumina before grinding; Figs 13(b) and 13(c) show surfaces after grinding experiments in 6  $\mu\text{m}$  slurry under 450 N and 900 N, respectively. The grinding direction is from bottom right to top left. Both ground surfaces show the same features characteristic for grinding. Surface grooves are in the direction of grinding and their size (depth and width) is proportional to the applied load. The

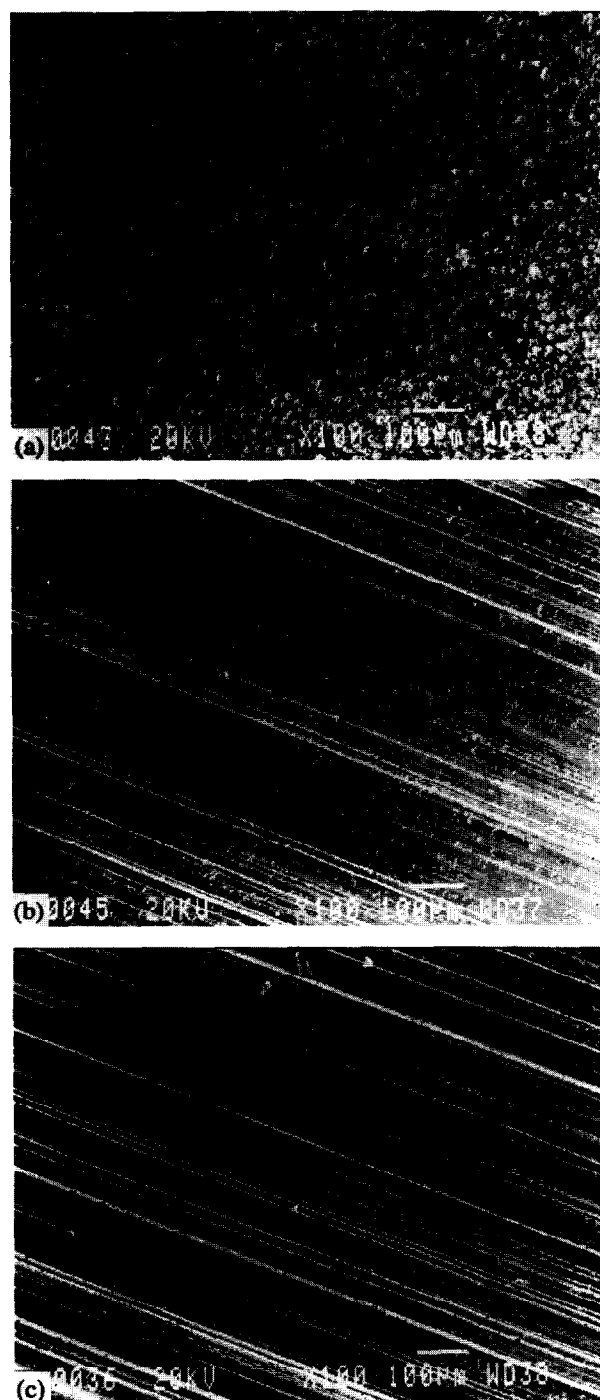


Fig. 13. SEM micrographs of alumina surfaces: (a) before grinding experiment; (b) after grinding experiment at 450 N; (c) after grinding experiment at 900 N. Diamond slurry with 6  $\mu\text{m}$  particles; rotational velocity of the ceramic pin, 300 rev min<sup>-1</sup>; duration of the test, 60 min.

deeper and wider the grooves, the higher the material removal rate. It can also be said that the high material removal rate is associated with rather poor surface finish.

### 4.2 Role of diamond particle size in material removal process

It is well known that the rate of material removal depends on the size of abrasive particles used and usually increases with the increase in their size.<sup>7,8</sup>

In this study, however, it was found that the above trend is not exactly observed. As can be seen in Figs 2 and 8, the rate of material removal is clearly lower for 25  $\mu\text{m}$  diamond particles than for 15  $\mu\text{m}$  particles, at which a maximum rate was recorded. This is true for both alumina and sialon.

To provide some explanation for this trend in material removal, it is helpful to consider the number of diamond particles per unit volume of the slurry as this seems to be an important parameter governing the grinding process. It can be easily shown that, on average, in a unit volume of 1  $\mu\text{m}$  slurry there are approximately 16 000 more diamond particles than in the same unit volume of 25  $\mu\text{m}$  slurry.<sup>7</sup> It follows then that 1  $\mu\text{m}$  diamond slurry should give higher material removal rates due to the larger number of diamond particle-ceramic rod contacts per unit time than in the 25  $\mu\text{m}$  slurry. This, however, should be considered in conjunction with possible hydrodynamic effects within the contact area. As there is no direct evidence in support of the explanation given below, therefore it must be regarded as only hypothetical.

The load, speed, grinding slurry liquid and contact geometry could have created conditions under which 15  $\mu\text{m}$  particles were able to enter the contact between the V-block and the ceramic rod and be embedded there, because the fluid film created by the hydrodynamic action was of an appropriate thickness. In case of 1  $\mu\text{m}$  and 6  $\mu\text{m}$  particles the fluid film was apparently too thick, so that they passed through the contact zone without removing much of the material. On the other hand, the fluid film thickness created under similar conditions of load, speed and contact geometry must have been too small for the 25  $\mu\text{m}$  particles so they could not easily enter the contact zone. Hence the material removal rates recorded are significantly lower.

For a high rate of material removal to be achieved during a grinding experiment it was essential that diamond particles could gain easy access to the contact zone and stay there. The retention of particles in the contact zone is only possible if they can embed into the counterface. Figure 14 shows SEM micrographs of the mild steel counterface after grinding experiments on sialon in 6 and 25  $\mu\text{m}$  slurries. It is clearly seen on both micrographs that diamond particles entered the counterface. However, it seems that 6  $\mu\text{m}$  particles penetrated the counterface much more easily and, more importantly, are embedded more firmly [Fig. 14(a)] than 25  $\mu\text{m}$  particles [Fig. 14(b)]. This can be justified by the number of diamond particles seen on the micrographs shown in Fig. 14. A direct consequence of that could be the decrease in material removal rate observed.

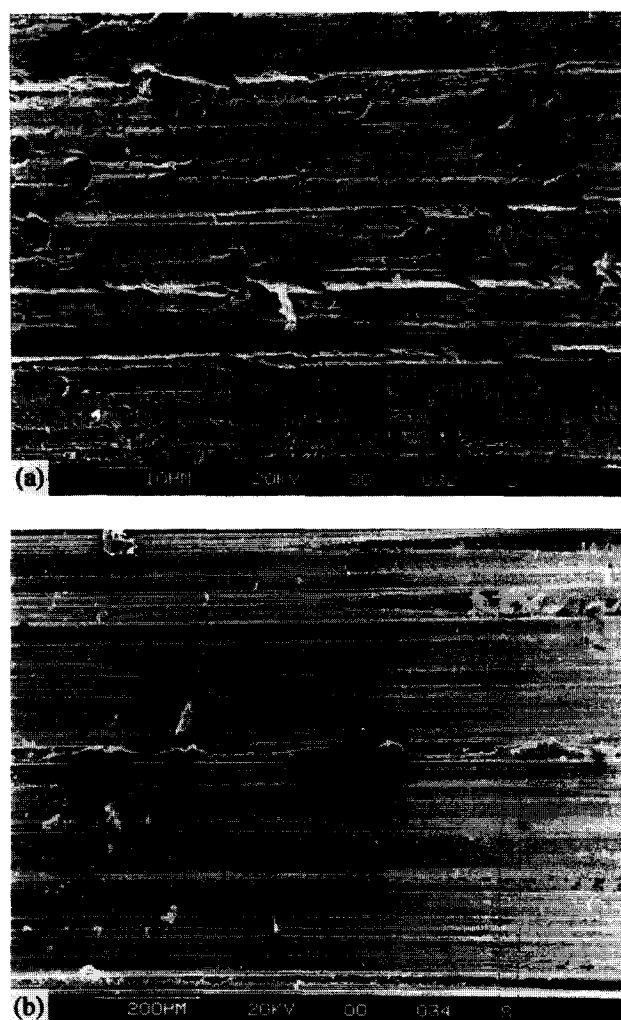


Fig. 14. SEM micrographs of the mild steel counterface after grinding experiment at 900 N and 300 rev min<sup>-1</sup>; (a) 6  $\mu\text{m}$  slurry; (b) 25  $\mu\text{m}$  slurry.

#### 4.3 Counterface materials

It is clear from Figs 5 and 8 that the counterface material has a considerable effect on the removal rate. In an attempt to explain this, the counterface surface after grinding experiments on sialon in 15  $\mu\text{m}$  diamond slurry at the load of 900 N was examined under a microscope. The results are shown in Figs 15(a) and 15(b) for mild steel and aluminium counterfaces, respectively.

Figure 16 shows the changes in hardness of steel and aluminium counterfaces after a grinding experiment on alumina in 6  $\mu\text{m}$  diamond slurry. It is seen that the surface of the aluminium counterface is considerably harder than its interior [Fig. 16(a)]. The decrease in hardness takes place over the depth of almost 200  $\mu\text{m}$ , after which the hardness remains constant. This points to an appreciable work-hardening of aluminium occurring during grinding and is supported by findings from abrasive wear tests reported by Gahr-Zum.<sup>9</sup> On the other hand, the hardness of the steel counterface does not change at all as evidenced by the results presented in Fig. 16(b).

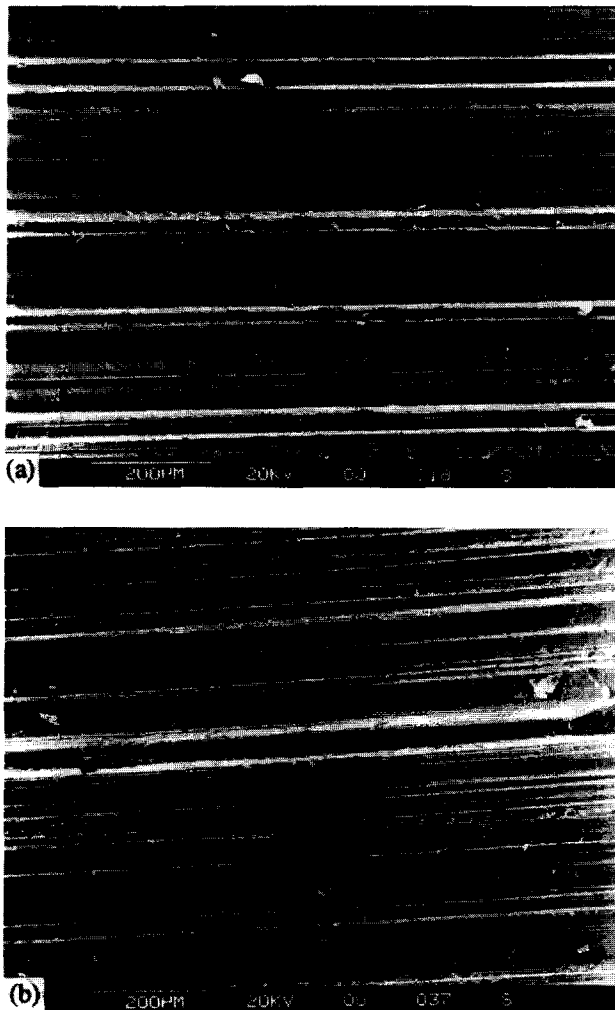


Fig. 15. SEM micrographs of counterface surfaces after grinding experiment at 900 N and 300 rev min<sup>-1</sup> in 6  $\mu$ m slurry: (a) mild steel; (b) aluminium alloy.

It could therefore be argued that diamond particles penetrate the aluminium counterface much more easily and have a better chance to be retained by the counterface due to a significant work-hardening effect. This is apparently not the case with the steel counterface. It is not only harder than the aluminium counterface (more difficult ingress into the material for diamond particles) but it also does not undergo any work-hardening, resulting in a poor retention of diamond particles. This is believed to be the main reason why the aluminium counterface is more effective in material removal than the mild steel one.

The third counterface material used during grinding experiments was brass, which was characterized by the lowest hardness among the materials tested. It also gave the lowest material removal rates (see Fig. 5). Figure 17 shows optical images of the cross-section through the brass counterface after a grinding test on alumina in 6  $\mu$ m diamond slurry. It can be clearly seen that the outermost layer has a different structure than the bulk material. Microhardness measurements

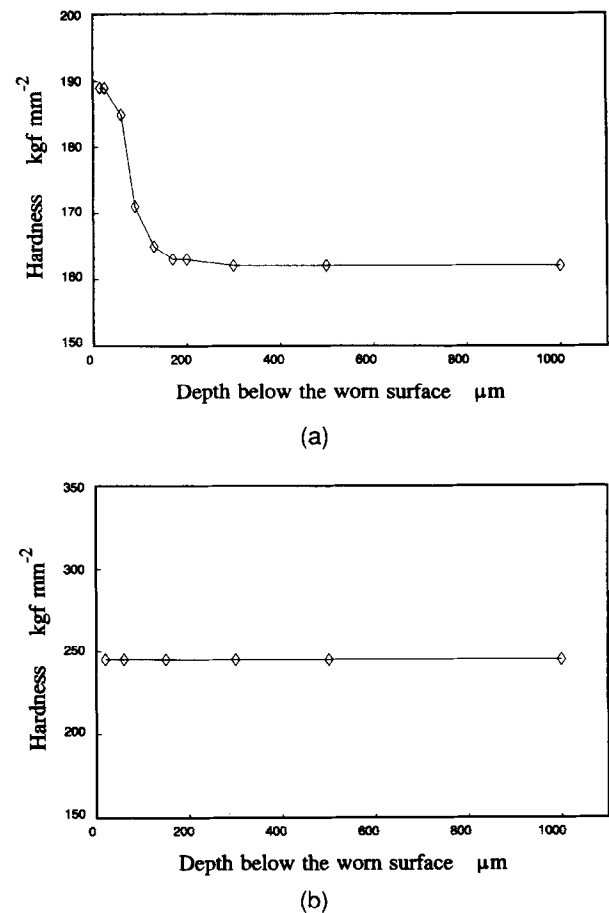


Fig. 16. Hardness profile of counterfaces after grinding experiment at 900 N and 300 rev min<sup>-1</sup> in 6  $\mu$ m slurry: (a) mild steel; (b) aluminium alloy.

revealed that this top layer is softer than the bulk material. In the context of material removal rate it means that this relatively soft layer of material could have acted as a solid lubricant, preventing embedded diamond particles from remaining in the contact zone. As a result, a low rate of grinding was observed.

## 5 Conclusions

The results presented in this paper lead to the following conclusions.

- (1) The rate of wear of alumina and sialon in sliding contact depends on the size of the abrasive particles and the counterface material.
- (2) The highest wear rates were achieved for the aluminium counterface followed by the mild steel counterface. The lowest wear rates were obtained for the brass counterface.
- (3) Grinding in 15  $\mu$ m diamond slurry consistently resulted in high material removal rates.
- (4) The rate of material removal increases with an increase in the applied load on the contact.

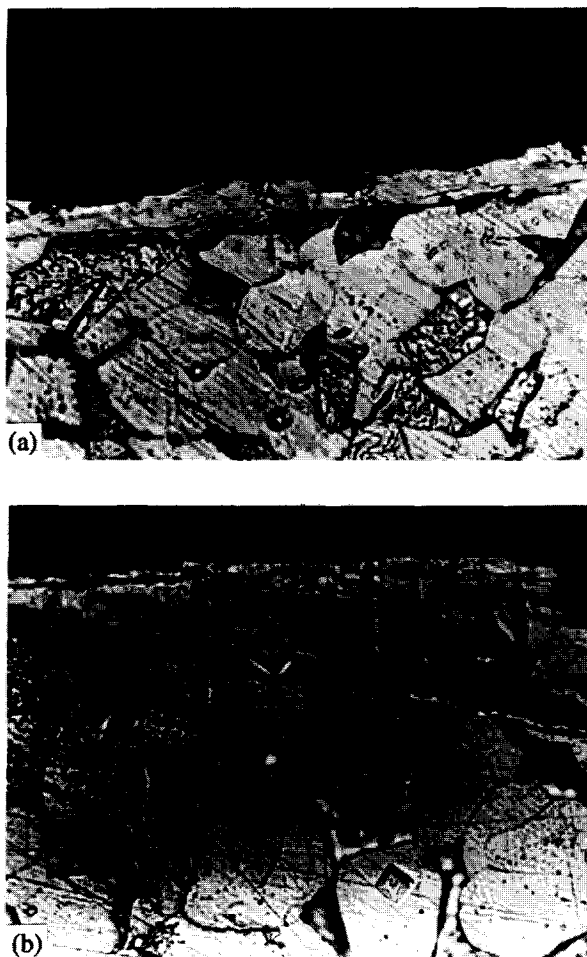


Fig. 17. Optical micrographs of the cross-section through the brass counterface after grinding experiment at 900 N and 300 rev min<sup>-1</sup> in 6  $\mu$ m slurry.

- (5) The roughness of ground surfaces increases with an increase in the material removal rate.

### Acknowledgements

The authors would like to thank the Engineering and Physical Science Research Council and the Defence Research Agency, who jointly funded this research, for permission to publish this paper.

### References

1. Wang, J. C. & Hus, S. M., Chemically assisted machining of ceramics. *Trans. ASME J. Tribol.*, **116** (1994) 423.
2. Malkin, S. & Ritter, J. E., Grinding mechanisms and strength degradation for ceramics. *J. Eng. Ind.*, **111** (1989) 167.
3. Rezaei, S. M., Sato, T., Waido, T. & Noguchi, H., Creep feed grinding of advanced ceramics. *Proc. IMechE, J. Eng. Manuf.*, **206** (1992) 93.
4. Van der Berg, P. H. J., Strength and residual stress of Mg-PSZ after grinding. *Wear*, **160** (1993) 301.
5. Kato, K., Tribology of ceramics. *Wear*, **136** (1990) 117.
6. Childs, T. H. C., Jones, D. A., Mahmood, S., Zhang, B., Kato, K. & Umehara, N., Magnetic fluid grinding mechanics. *Wear*, **175** (1994) 189.
7. Stolarski, T. A., Jisheng, E., Gawne, D. T. & Panesar, S., The effect of applied load and abrasive particle size on the material removal rate of silicon nitride artefacts. *Ceram. Int.*, **21** (1995) 355–66.
8. Yamamoto, T., Olsson, M. & Hogmark, S., Three-body abrasive wear of ceramic materials. *Wear*, **174** (1994) 421.
9. Gahr-Zum, K. H., *Microstructure and Wear of Materials*. Elsevier, Amsterdam, 1987, p. 400.